Stereoacuity in the periphery is limited by internal noise

Susan G. Wardle School of Psychology, The University of Sydney, Sydney, New South Wales, Australia

Peter J. Bex Schepens Eye Research Institute, Department of Ophthalmology, Harvard Medical School, Boston, Massachusetts, USA

John Cass School of Psychology, University of Western Sydney, Sydney, New South Wales, Australia

David Alais School of Psychology, The University of Sydney, Sydney, New South Wales, Australia

It is well-established that depth discrimination is finer in the fovea than the periphery. Here, we study the decline in depth discrimination thresholds with distance from the fovea using an equivalent noise analysis to separate the contributions of internal noise and sampling efficiency. Observers discriminated the mean depth of patches of "dead leaves" composed of ellipses varying in size, orientation, and luminance at varying levels of disparity noise between 0.05 and 13.56 arcmin and visual field locations between 0° and 9° eccentricity. At low levels of disparity noise, depth discrimination thresholds were lower in the fovea than in the periphery. At higher noise levels (above 3.39 arcmin), thresholds converged, and there was little difference between foveal and peripheral depth discrimination. The parameters estimated from the equivalent noise model indicate that an increase in internal noise is the limiting factor in peripheral depth discrimination with no decline in sampling efficiency. Sampling efficiency was uniformly low across the visual field. The results indicate that a loss of precision of local disparity estimates early in visual processing limits fine depth discrimination in the periphery.

Keywords: stereoacuity, depth discrimination, equivalent noise analysis, stereopsis, peripheral vision

Citation: Wardle, S. G., Bex, P. J., Cass, J., & Alais, D. (2012). Stereoacuity in the periphery is limited by internal noise. *Journal of Vision, 12*(6):12, 1–12, http://www.journalofvision.org/content/12/6/12, doi:10.1167/12.6.12.

Introduction

The stereo resolution of the human visual system is remarkably fine under optimal conditions with thresholds for relative depth discrimination as low as a few seconds of arc (e.g., McKee, 1983; Rawlings & Shipley, 1969; Stevenson, Cormack, & Schor, 1989; Westheimer & McKee, 1980a, 1980b). The precision of stereopsis is important for quantitative depth perception and in segmenting natural scenes (Julesz, 1971; Wardle, Cass, Brooks, & Alais, 2010). Stereoacuity is typically quantified as the smallest detectable separation in depth between two stimuli. In the fovea, it is a hyperacuity; depth differences can be distinguished that are smaller than the diameter of individual photoreceptors (Howard, 1919; Westheimer, 1975, 1979; Westheimer & McKee, 1980a). Although larger absolute disparities can be detected in the periphery, stereoacuity is finest in the fovea and on the horopter, and declines both in the periphery and away from the fixation plane (Blakemore, 1970). Even a small disparity pedestal elevates depth discrimination thresholds (Westheimer, 1979).

Stereoacuity declines in the periphery along the horizontal (Rawlings & Shipley, 1969) and vertical (McKee, 1983) meridians compared to the fovea. It is preferable to measure peripheral sensitivity along the meridians as stereoacuity declines off the horopter. Rawlings and Shipley (1969) reported stereo thresholds at 8° eccentricity on the horizontal meridian that were around 16 times greater than that in the fovea. The falloff in performance is rapid; for the vertical meridian threshold elevation has been measured only a few minutes of arc from the fovea (McKee, 1983). Stereoacuity in the periphery falls off faster than resolution acuity (Fendick & Westheimer, 1983) indicating that it is not accounted for by the resolution limit of the retinal photoreceptors.

There is evidence that a change in the spatial scale of receptors across the visual field is related to the decline in stereoacuity in the periphery. When other hyperacuities are *M*-scaled to account for cortical magnification,

doi: 10.1167/12.6.12 Received February 29, 2012; published June 7, 2012

performance is comparable across the visual field (vernier acuity: Levi, Klein, & Aitsebaomo, 1985; Virsu, Näsänen, & Osmoviita, 1987). Siderov and Harwerth (1995) measured depth discrimination for difference of Gaussian stimuli of various spatial frequencies at a range of eccentricities and pedestal disparities off the horopter. Thresholds were higher with increasing crossed or uncrossed pedestal disparities, independent of spatial frequency and retinal eccentricity. However, thresholds at different eccentricities were found to be dependent on spatial frequency. For low spatial frequencies (0.5 c/°), discrimination performance was relatively invariant as a function of retinal eccentricity within the range tested, up to 10°. However, for higher (2 and 8 c/°) spatial frequency stimuli, performance declined rapidly with eccentricity. The authors suggest that low frequency mechanisms are consistently placed across the retina, thus stereoacuity for low spatial frequencies is invariant with eccentricity. As stereoacuity declined rapidly with eccentricity for higher spatial frequencies, they suggest that either the number of high frequency mechanisms declines with eccentricity or, in the periphery, stimuli are detected by a nonoptimal mechanism tuned to a lower frequency. Spatial scale cannot account for how the increase in receptive field size degrades performance, thus the reason for the decline in stereoacuity in the periphery remains unclear.

Reduced peripheral stereoacuity is likely to be either a consequence of an increase in the bandwidth and size of disparity-tuned mechanisms or a decrease in their number and density across the visual field. Neurophysiological differences between foveal and peripheral vision begin within the retina. The density of cones and ganglion cells in the human retina falls off with eccentricity (Curcio & Allen, 1990; Curcio, Sloan, Kalina, & Hendrickson, 1990), suggesting coarser sampling in the periphery (see Snyder, 1982). However, the optics of the human eye remain nearly constant over a large region of around 10° centered on the optical axis (Jennings & Charman, 1981). It is established that the receptive field size of neurons in striate cortex increases with eccentricity, particularly for complex cells (cat: Wilson & Sherman, 1976). Disparity tuning in V1 is coarser and wider (Prince, Cumming, & Parker, 2002) for the periphery with a larger standard deviation in receptive field disparity (Joshua & Bishop, 1970). Natural scene statistics reveal a similar pattern to these V1 cells. The standard deviation of the distribution of disparities in natural scenes increases in the periphery relative to a virtual observer (Liu, Bovik, & Cormack, 2008). Together, these results suggest that the local estimates of disparity are likely to be noisier in the periphery, thus precision in locating each element in depth, and hence stereoacuity, is reduced. It may also be that there are fewer disparity-tuned mechanisms with peripheral receptive fields. In this case, undersampling of disparity by a coarser representation of space in the peripheral visual field may also increase noise in the estimates.

In this paper, our aim is to use equivalent noise analysis (Barlow, 1956) to parse out the relative contributions of these factors to the decline of stereoacuity in peripheral vision. We will measure the depth increment threshold (smallest detectable difference in disparity that can be detected between two stimuli) at different locations in the visual field. The method of equivalent noise (e.g., Allard & Faubert, 2006; Dakin, Bex, Cass, & Watt, 2009; Dakin, Mareschal, & Bex, 2005a, 2005b; Heeley, Buchanan-Smith, Cromwell, & Wright, 1997; Lu & Dosher, 1999) will be used to weigh the relative contributions of sampling and internal noise, as explained in this article.

Equivalent noise analysis uses additivity of variance to partition out the sources of noise that contribute to observed psychophysical thresholds. The advantage of this method is that it can help clarify why thresholds differ across conditions. The observed threshold corresponds to the sum of external and internal noise divided by the number of samples (Equation 1). The (squared) observed threshold is a sampling distribution; thus the sum of the two sources of variance (internal and external noise, which are assumed to be normally distributed) is divided by N, which corresponds to the number of samples and is proportional to sampling efficiency (Solomon, 2010). The core assumption of the model is that internal noise for any set of conditions is a constant. Performance at low levels of external noise is jointly determined by internal noise and sampling. However, when the level of external noise greatly exceeds internal noise, the contribution of internal noise becomes minimal, and thresholds depend primarily upon sampling efficiency. External noise can be manipulated experimentally by increasing the variance in the stimulus along the parameter of interest. In this case, the level of external noise corresponds to the standard deviation of the distribution of binocular disparities in the stimulus. Psychophysical thresholds are measured under increasing levels of external noise (disparity variance) and across different conditions (degrees of eccentricity). This allows for comparison of these sources of error across different eccentricities. The two-parameter model (internal noise and number of samples) is fitted to the thresholds across levels of external noise, estimating the contribution of each to the observed thresholds.

We will use two clusters of ellipses generated from a "dead leaves" model as our stimuli for depth discrimination (e.g., Lee, Mumford, & Huang, 2001; Lindgren, Hurri, & Hyvärinen, 2008; Ruderman, 1997; Srivastava, Lee, Simoncelli, & Zhu, 2003). As far as we are aware, dead leaves have not been used in a stereopsis

experiment before, however, they have been used in computational analysis of binocular images (Aschenbrenner, 1954; Langer, 2008). The advantage of these stimuli is that they have properties similar to natural images; are varied in size, luminance, contrast, and orientation; and allow for manipulation of disparity variance by individually assigning the disparity of each ellipse.

Figure 1 illustrates the predictions of the two-parameter equivalent noise model for a schematic version of our stimuli. For clarity, only a few individual ellipses at different disparities are shown. The two sources of behavioral variability (internal noise and sampling efficiency) predict different causes for the decline in depth discrimination with increasing stimulus eccentricity. If local estimates of disparity are noisier in the periphery, the estimate of internal noise (σ_{int}) will rise with eccentricity (Figure 1a). In this case, the disparity of each individual stimulus element is more uncertain in the periphery compared to the fovea. Similarly, if a coarser representation of space causes undersampling in the periphery, lower estimates of the number of samples (N) will be observed further from the fovea (Figure 1c). Here, the loss of precision is caused by a reduction in the pooling of the disparities of individual local elements.

$$\sigma_{obs}^2 = \frac{\sigma_{\text{int}}^2 + \sigma_{ext}^2}{N} \quad (1)$$

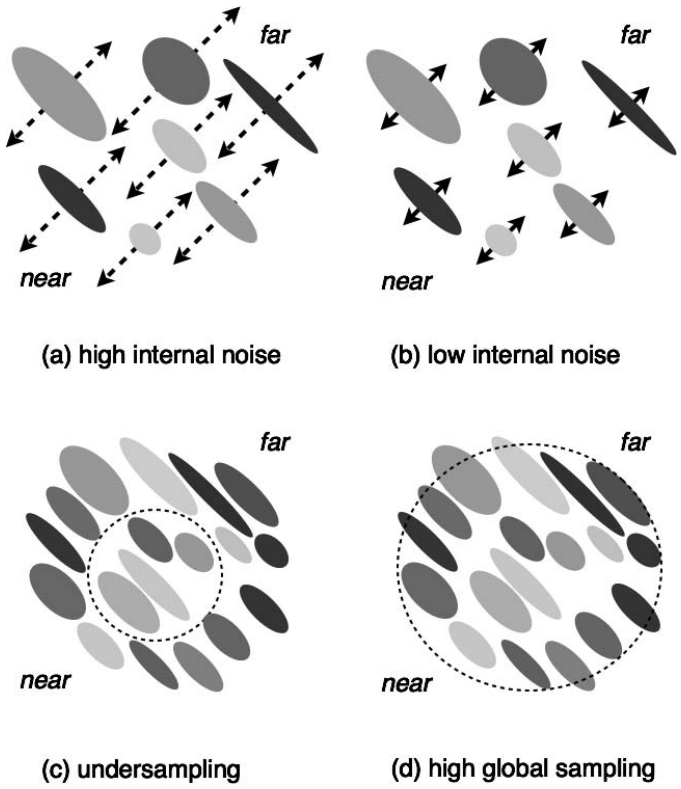

Figure 1. Schematic representation of internal noise (top row) and number of samples (bottom row) in the equivalent noise model. Ellipses represent the individual stimulus elements used in the experiment, which are at different depths. Depth in each panel is shown along the diagonal axis, from near-depth in the bottom left corner to far-depth in the top right corner. *x* and *y* axes for each panel are the stimulus locations relative to the observer, to the right (bottom right of each panel) and left (upper left of each panel). (a) At high levels of internal noise, precision in locating each element in depth is reduced (indicated by the dashed arrows). (b) At low levels of internal noise, the location of each element in depth is more precise. (c) If the global depth is undersampled, only a few elements are pooled, compared to (d) a higher sampling rate.

Methods

Observers

Three observers with normal stereovision and normal or corrected-to-normal visual acuity participated. Two were authors (SW and JC) and the third was a senior undergraduate student (SG) who was naive to the aims of the experiment and reimbursed for participation at the rate of $20/hr. The experiment was conducted in accordance with the Declaration of Helsinki.

Stimuli

Stimuli were generated on a PC using MATLAB (The MathWorks) with functions from the Psychtoolbox (Brainard, 1997; Pelli, 1997). Stimuli were presented on a Viewsonic VX2268wm LCD monitor at 120 Hz with screen resolution 1680 × 1050 pixels. Shutter glasses (Nvidia GeForce 3D Vision) were used to control stereoscopic stimuli presentation. The 120 Hz monitor alternated between each eye's view, updating at 60 Hz per eye. The (LCD) monitor was gamma-corrected to obtain linear output across RGB values. Subpixel resolution via the graphics card provided a spatial positioning accuracy of .004 pixel, corresponding to a stereo display resolution of 0.2 arcsec.

The stimuli for depth discrimination were two patches of "dead leaves" (Lee, Mumford, & Huang, 2001; Ruderman, 1997) constructed from ellipses that differed in luminance, size, and orientation (see Figure 2). Each square patch contained 200 ellipses; one patch served as the test stimulus and the other as the reference stimulus. The number of ellipses was intended to fill the entire stimulus area with no visible background and, as a result, many of the ellipses were wholly or partially occluded. The patches measured approximately 3° × 3° of visual angle and were placed one above the other

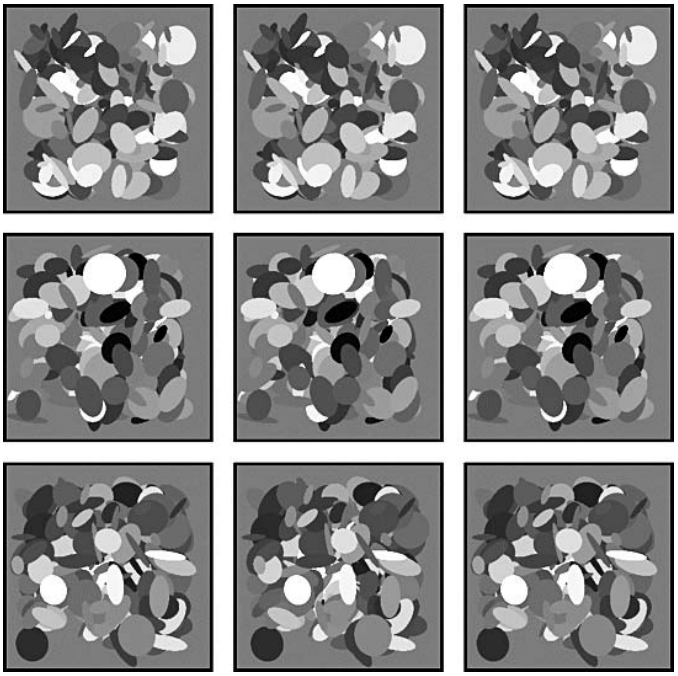

Figure 2. Examples of the stimuli at disparity noise levels $SD =$ 0.05 (top row), 3.39 (middle row), and 9.44 (bottom row) arcmin. These disparities are for the stimulus size and viewing distance in the experiment, and are not scaled in the diagram. The left and middle column is for crossed fusion, and the middle and right column for uncrossed fusion. A unique set of ellipses was generated for each trial. The examples shown here are not gamma-corrected, so they differ in luminance and contrast from the experimental stimuli.

separated by an average distance of 16.9 arcmin with the reference patch always on the bottom. The screen location of each ellipse was randomly drawn from a uniform distribution of dimensions within the stimulus space; therefore, the measurement of the stimulus border is approximate as the edges of some ellipses fell outside this area. The luminance distribution of the elements was drawn from a distribution whose skew and kurtosis were matched to the statistics of the McGill natural image database (Olmos & Kingdom, 2004) and RMS contrast was 0.32. The height and width of each ellipse was determined by uniformly distributed random values between 6.8 and 54.2 arcmin. The luminance and size of each ellipse was selected at the start of the experiment and was constant for all trials in the session. However, the orientation, screen location, and disparity of each ellipse was randomly allocated on each trial. This means that the stimuli were unique for each trial, and an ellipse that was in the reference patch for one trial could be in the test patch for another trial.

The binocular disparity of each ellipse was randomly selected from a normal distribution with a fixed mean and standard deviation. The standard deviation determined the level of external (disparity) noise and was equal in the test and reference patch for each noise level. The mean disparity of the ellipses in the reference patch was always set at zero, and the mean disparity of the ellipses in the test patch was varied to determine the depth discrimination threshold using the method of constant stimuli as explained in Procedure. Each ellipse was shifted horizontally in the other eye's image to produce disparity and the perception of depth. The patches appeared as square-shaped clusters of ellipses; each ellipse had an individual disparity centered on the mean disparity. Disparity was relative to the screen rather than the observer's horopter because the stimulus locations were along the horizontal meridian of the visual field as in Rawlings and Shipley (1969). At the viewing distance used, the distance of each of the peripheral screen locations from the theoretical horopter was 0.079° at 3° eccentricity, 0.315° at 6° eccentricity, and 0.706° at the greatest eccentricity of 9°.

In these stimuli, transparency is sometimes perceived in the overlapping ellipses for certain combinations of luminance and depth order (e.g., Nakayama & Shimojo, 1992). This can alter the perceived depth of a particular ellipse, which means that the perceived depth may not equal the disparity assigned to that element from the normal distribution of disparity noise. As both screen location and disparity were randomly assigned to each ellipse on every trial, any change in perceived depth for some of the stimulus elements would not be systematic across trials. This has the effect of adding uniform noise to the disparity signals, but does not change the shape of the underlying disparity distribution. Additionally, the presence of transparency could not be used as an alternative cue for discrimination between the stimuli as it is equally likely to occur in the test and reference patches of ellipses.

Procedure

Observers completed a short training program to test that their stereovision was adequate for the task before they began the main experiment. In the training program, observers were shown two patches of dead leaves with all ellipses at the same disparity, i.e., standard deviation $SD = 0$ or at a moderate level of noise $SD = 3.39$ arcmin. The reference patch was always at zero disparity, and the test patch was at either crossed or uncrossed disparity. On each trial, observers identified whether the test patch was closer or further than the reference patch. Observers practiced the task at the fovea and at the greatest eccentricity tested (9°). As stereo thresholds improve with practice, particularly for stimuli in the periphery (Fendick & Westheimer, 1983), care was taken to ensure thresholds had

stabilized in each observer before data collection commenced.

Observers wore shutter glasses and were seated 114 cm from the computer monitor with their position fixed using a chin and forehead rest. The experimental room was painted black, and the only illumination came from the computer monitor. Vergence was maintained at zero disparity with nonius lines and a short stimulus duration. Each trial began with the presentation of a black nonius cross (line length: 50.8 arcmin; line width: 3.4 arcmin) with a binocular horizontal line and monocular vertical segments. The cross was vertically centered between the stimulus locations and was flanked by two pairs of black and white vertical nonius lines (length: 1.4°; width: 6.8 arcmin; vertical separation: 10.2 arcmin; horizontal separation: 50.8 arcmin). The upper and lower segments of the lines were presented to opposite eyes and, when fused, they appeared as two vertical lines, one black and the other white.

The observer pressed a key to initiate each trial when the nonius lines and cross appeared aligned, indicating that their eyes were converged at zero disparity. The nonius lines and cross only appeared in-between trials, and were replaced by a square fixation point (11.9 × 11.9 arcmin) when the stimuli were displayed. The stimuli were presented for 200 ms, too brief to allow for the completion of a vergence eye movement away from the fixation plane (McKee, Bravo, Taylor, & Legge, 1994). The observer pressed a button to indicate whether the test patch (above fixation) or reference patch (below fixation, always at zero disparity) was closer in depth. The allocation of crossed or uncrossed disparity to the test patch was random on each trial, resulting in an absolute depth discrimination threshold from zero, which did not consider the sign of the disparity. Feedback was given by changing the color of the horizontal line of the nonius fixation cross to green (correct) or red (incorrect) for 200 ms.

The stimuli were centered either on the fovea (0°), 3°, 6°, or 9° eccentricity to the right of fixation along the horizontal meridian. The stimuli extended approximately 1.5° in each direction from the center. As each stimulus patch was 3° × 3° in size and separated vertically from each other by 16.9 arcmin, these values reflect the location of the middle of the stimulus in the horizontal direction rather than the minimum gap between the fovea and the edges of the stimulus patches. It was checked that none of these locations fell in the observer's blind spot where there is no binocular vision by a short blind spot mapping program. Observers moved a small yellow disc around the screen to locate their blind spot and ensure it did not overlap with any of the stimulus display locations. Eight levels of external disparity noise were used in log-spaced steps: 0.05, 0.21, 0.42, 0.85, 1.69, 3.39, 6.78, and 13.56 arcmin. This resulted in 32 (four eccentricities × eight levels of external noise) separate conditions.

The method of constant stimuli was used to determine the depth discrimination threshold for each condition. The mean disparity of the ellipses in the test patch was varied in 17 evenly spaced steps starting at zero in order to determine the depth discrimination threshold. The step size was determined from pilot testing for each eccentricity and noise level in order to adequately sample the psychometric function. Each mean disparity of the test stimulus was repeated a minimum of 20 times over two or more runs, so each threshold was calculated from a minimum of 340 trials. Each run combined at least two levels of external noise so that the reference stimulus was not the same on each trial. Consequently, observers could not use their response on the previous trial to gauge their answer as the reference stimulus was usually different. The eccentricity conditions were completed in separate runs with each run containing only one eccentricity.

Threshold estimation

Psychometric functions were obtained by fitting a cumulative Gaussian function to the data for each condition using the Levenberg-Marquardt algorithm implemented with Matlab's *nlinfit* routine. The standard deviation of the fitted function was taken as the threshold estimate. Confidence intervals (95%) on the threshold estimates were derived from the Jacobian matrix of the fitted function with Matlab's *nlparci* routine.

Equivalent noise model

The equivalent noise model (Equation 1) was fitted to each observer's data with the Levenberg-Marquardt algorithm. A separate fit was calculated for each of the four eccentricities for each observer. The fit was weighted using the confidence intervals for the psychometric functions. Confidence intervals (95%) were estimated for the fitted parameters of internal noise (σ_{int}) and sampling efficiency (N) using the method previously described for the psychometric functions.

Results

Depth discrimination thresholds as a function of disparity noise level and visual field location are shown individually for each observer in Figure 3. The equivalent noise fits (Equation 1) for each eccentricity are plotted as solid lines. Naive observer SG was unable

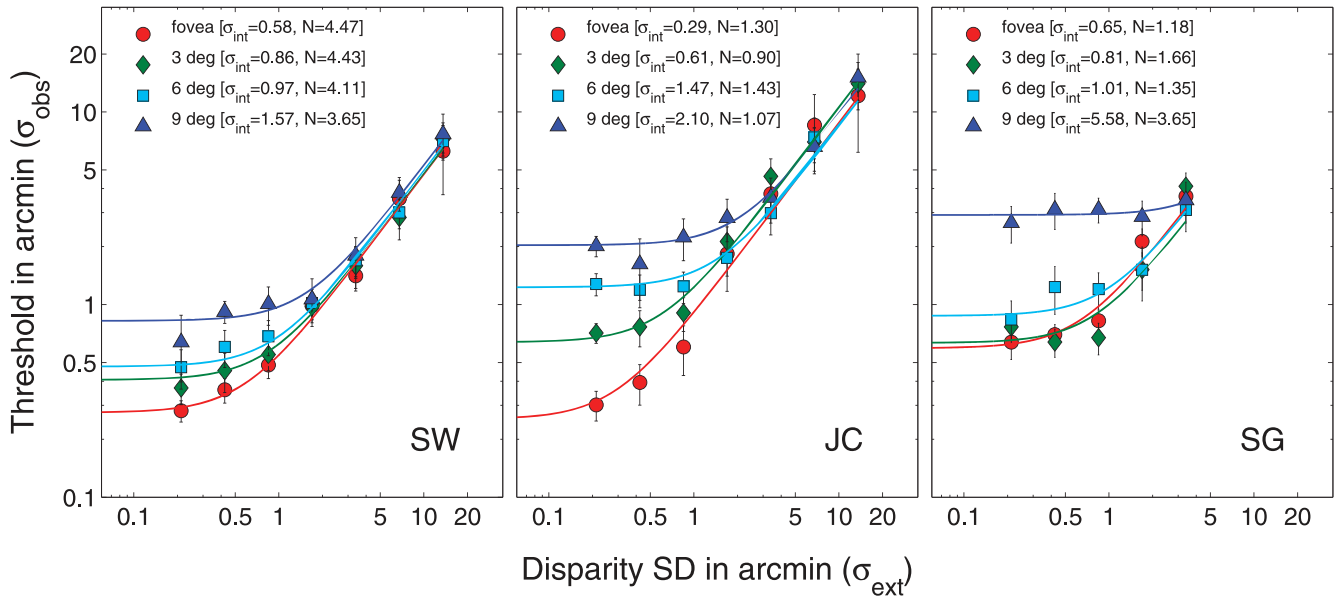

Figure 3. Depth discrimination thresholds as a function of disparity noise (σ_{ext}) and visual field location for three observers. Solid lines show equivalent noise fits (Equation 1) for each eccentricity. Parameter estimates for internal noise (σ_{int}) and sampling efficiency (N) are in the legend. Error bars are 95% confidence intervals on the threshold estimates.

to perform the depth discrimination task at the two highest levels of disparity noise ($SD = 6.78$ and 13.56 arcmin) so, for this observer, the equivalent noise functions were fit to the remaining six noise levels. One threshold for observer JC (6° eccentricity, $SD = 13.56$ arcmin) could not be estimated from the data, so this point was excluded from the equivalent noise analysis. Overall, for each eccentricity, discrimination thresholds are lowest at the smallest levels of disparity noise and increase with greater levels of disparity noise. Across observers, at the lowest noise level, thresholds in the fovea range from 0.27 to 0.64 arcmin, 0.44 to 0.80 at 3°, 0.39 to 1.39 at 6°, and 0.80 to 3.09 at 9°. At the sixth noise level ($SD = 3.39$ arcmin), thresholds converge across eccentricity for all three observers. At this level of noise, thresholds were in the range 1.41 to 3.76 arcmin in the fovea, 1.59 to 4.64 at 3°, 1.70 to 3.11 at 6°, and 1.80 to 3.59 at 9°.

The equivalent noise fits shown in Figure 3 reveal that, at lower levels of noise, thresholds for depth discrimination are lowest in the fovea and increase at further retinal eccentricities. However, for higher levels of disparity noise, the fits for each eccentricity converge so that there is minimal difference in thresholds across the visual field, and thresholds rise in proportion with external noise. There is considerable variability in the magnitude of the thresholds across observers; however, the overall pattern of convergence around 3.39 arcmin of noise is consistent. This pattern of threshold elevation indicates that internal noise is the limiting factor for depth discrimination in the periphery with little or no reduction in the sampling efficiency.

The parameter estimates of internal noise (σ_{int}) and sampling efficiency (N) from the individual equivalent noise fits are plotted separately in Figure 4. Data for observer SG at the greatest eccentricity (9°) is omitted from this figure and further analysis because a reasonable parameter estimate could not be obtained

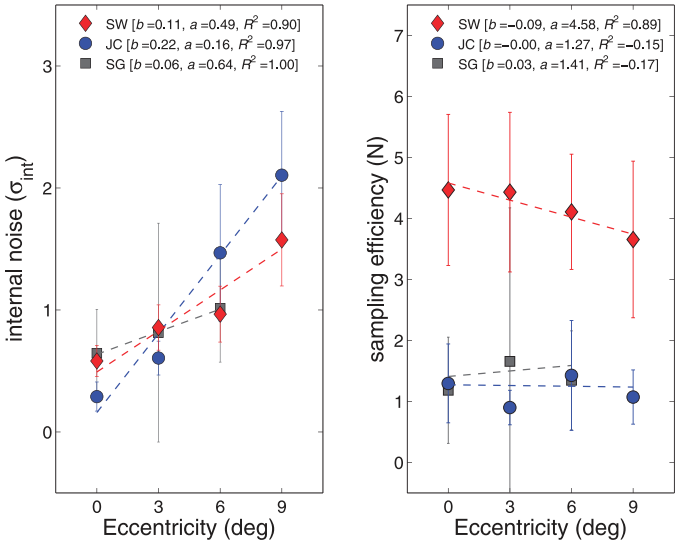

Figure 4. Parameter estimates for internal noise (σ_{int}) and sampling efficiency (N) as a function of visual field eccentricity for three observers. Dashed lines are linear fits to the data using weighted least-squares, fitted parameters for the slope (b) and intercept (a) are shown in the legend. Data for observer SG at 9° eccentricity are omitted because reasonable parameter estimates could not be obtained for this condition (see text for details). Error bars are 95% confidence intervals.

for this condition. Parameter estimates for SG at 9° as shown in Figure 3 are 5.58 (95% CI: [−0.2, 11.4]) for σ_{int} and 3.65 [95% CI: −3.5, 10.8] for N. As apparent in Figure 3, thresholds for SG at 9° eccentricity do not appear to vary with noise level, so observer SG's data is only considered from the fovea to 6° eccentricity.

For all three observers, internal noise increases with increasing visual field eccentricity with higher internal noise in the periphery. The magnitude is approximately a 2.7-fold increase for SW, a 7.2-fold increase for JC, and a 1.6-fold increase for observer SG (from the fovea to 6°). However, there is no systematic change in sampling efficiency with eccentricity. If a reduction in sampling efficiency were driving the increase in depth discrimination thresholds in the periphery, a reduction in N would be expected in the periphery compared to the fovea. However, the estimates of N remain approximately constant across eccentricity for all observers with a difference of only 0.82 (SW), 0.52 (JC), and 0.48 (SG, from the fovea to 6°) between the maximum and minimum estimates of N.

In order to obtain a quantitative estimate of the change in internal noise and sampling efficiency with eccentricity, a first-order polynomial in the form $y = a + bx$ was fit to the parameter estimates using weighted least-squares. The fits are represented as the dashed lines in Figure 4 with the best-fitting parameters for the slope (b) and intercept (a). For all observers, there is a positive slope for the fit to internal noise across eccentricity (b = 0.11, 0.22, and 0.06 for observers SW, JC, and SG, respectively). R^2 was in the range 0.90 to 1.00 for all observers. This means that, for each degree increase in eccentricity, internal noise rose by 0.06 to 0.22 arcmin across observers. The linear fits to sampling efficiency were poorer with uniformly low estimates of b ($b = -0.09$, 0, and 0.03 for observers SW, JC, and SG, respectively). Corresponding R^2 for the fits were 0.89, −0.15, and −0.17, respectively, indicating poor fits except for observer SW. Apart from a small effect for observer SW, the fitted functions reveal no change in sampling efficiency with visual field eccentricity.

Discussion

We used equivalent noise analysis to examine the relative contribution of internal noise and sampling efficiency to the reduction in stereoacuity across the visual field. Observers discriminated the mean depth of patches of "dead leaves" at varying levels of external disparity noise. At low levels of noise, depth discrimination thresholds were lowest in the fovea and increased at greater eccentricities. At higher levels of disparity noise, thresholds were comparable across the visual field. Equivalent noise analysis indicated that the reduction in stereoacuity in the periphery was driven by an increase in internal noise with no evidence for a change in sampling efficiency.

Stereoacuity across the visual field

Previous investigations of stereoacuity have reported smaller thresholds than those in the present study. In the fovea, stereoacuity thresholds are less than 5 arcsec under optimal conditions (McKee, 1983) and can be as small as vernier thresholds (Westheimer & McKee, 1979). McKee (1983) measured stereoacuity using bar stimuli and found greatest sensitivity when the length of the bars was between 10 to 15 arcmin. However, estimates of stereoacuity are known to vary considerably with the stimuli and task used. Stevenson, Cormack, and Schor (1989) used random-dot stereograms to measure stereoacuity for different 2AFC depth discrimination tasks. The lowest thresholds of 1.7 to 3.6 arcsec across observers were reported for a task requiring the detection of which interval contained a depth step (a difference in depth between the lower and upper half of the dot field). Thresholds were considerably higher (22 to 38 arcsec) when the task involved discriminating a difference in depth (or thickness) between two overlapping random dot planes. The highest thresholds (136 to 351 arcsec) were obtained for a gap-resolution task, which required detection of a gap between two disparity planes compared to a "filled" thick plane of dots with equal thickness in depth.

In the present study, thresholds in the fovea for the lowest noise condition ($SD = 0.05$ arcmin) ranged from 16.46 to 38.28 arcsec across observers, which is comparable to thresholds for detecting a difference in depth between two overlapping random dot planes (Stevenson, Cormack, & Schor, 1989). This indicates that depth discrimination thresholds for our stimuli were outside the hyperacuity range but within the range of other depth discrimination tasks. This is expected because our stimuli were complex, containing a range of orientations, luminance, and sizes. The task also required the global averaging of the local disparity of the ellipses in the two stimulus patches although, at the lowest noise level, this would be negligible. The two patches had to be matched across an average vertical distance of 16.9 arcmin, although the borders of some ellipses within each patch would be closer because their locations were randomly generated. Stereoacuity thresholds double at an eccentricity of only 30 arcmin from the fovea (McKee, 1983), thus on average the stimulus placement in our foveal condition was already outside the range of the finest stereoacuity.

In agreement with previous literature, we found that stereoacuity thresholds increased with eccentricity

across the visual field. Rawlings and Shipley (1969) reported depth discrimination thresholds across the visual field on the horizontal meridian for 2 points (in stereo) of 21″ of arc at the fovea, 82″ at 2°, 155″ at 4°, 193″ at 6°, and 345″ at 8° eccentricity. These eccentricities are comparable to the ones in the present study; however, thresholds in the present study for the smallest noise level ($SD = 0.05$ arcmin) are considerably lower. In the fovea, thresholds across observers ranged from 16 to 38 arcsec, 26″ to 48″ at 3°, 24″ to 83″ at 6°, and 48″ to 185″ at 9°. The increase in thresholds between the fovea and the far periphery in Rawlings and Shipley (1969) was a ~16-fold increase compared to a group mean increase of ~5-fold in the present study. This discrepancy in threshold measurements may be explained by differences in the stimuli and method. Rawlings and Shipley's (1969) task required depth discrimination between two small point-light sources 60 arcsec in diameter. The dead leaves stimuli in the present study were much larger and subtended 3° × 3°. Our stimuli contained a greater distribution of disparity information. We demonstrate that the visual system is able to average disparity information, which could facilitate depth discrimination by an improved signal across multiple local cross-correlations. In addition, Rawlings and Shipley used a method of adjustment rather than a 2AFC task to measure thresholds. In their task, observers adjusted the separation of the two peripheral point targets until they appeared equidistant, and the threshold was taken as the mean deviation.

The stimuli used in this study were deliberately not equated for contrast, spatial frequency, or cortical magnification across the visual field because the aim was to use equivalent noise analysis to probe the decrement in stereoacuity thresholds in the periphery. Contrast sensitivity decreases with eccentricity (e.g., Rovamo, Virsu, & Näsänen, 1978), so it is possible that our stimuli were less visible when presented in the peripheral visual field. However, the luminance distribution of the dead leaves stimuli were matched to the distribution in natural scenes, calculated from a natural image database (Olmos & Kingdom, 2004), so there were local areas of both high and low contrast in the stimuli. When peripheral stimuli are *M*-scaled to equalize the cortical area stimulated, contrast sensitivity does not differ from the fovea (Rovamo, Virsu, & Näsänen, 1978). Although stereoacuity thresholds are lower at higher contrast, reducing stimulus contrast does not raise thresholds significantly until near contrast threshold, thus contrast would be unlikely to have an effect on stereoacuity for the suprathreshold stimuli in this experiment (Cormack, Stevenson, & Schor, 1991; Ogle & Weil, 1958).

Contrast sensitivity as a function of spatial frequency also changes with eccentricity. For low spatial frequencies, thresholds are lowest in the periphery and, for high spatial frequencies, maximum sensitivity is in the fovea (Virsu & Rovamo, 1979). Although the stimuli patches were the same size in the foveal and peripheral conditions, the individual ellipses varied in size and contrast. An ideal characteristic of these broadband stimuli is that a range of spatial frequency, luminance, and contrasts were available at all eccentricities. Siderov and Harwerth (1995) demonstrated with spatially narrowband difference-of-Gaussian stimuli that the decrease in depth discrimination performance in the periphery is limited to high spatial frequencies. Our data with spatially broadband stimuli indicate internal noise is the limiting factor in peripheral depth discrimination; the physiological implications of this are the focus of the next section.

Increase in internal noise with eccentricity

The fits of the equivalent noise model to our data indicate that the falloff in stereoacuity in the periphery is entirely due to an increase in internal noise. An analogous increase in directional internal noise has been shown to account for a reduction in direction discrimination thresholds in the peripheral visual field (Mareschal, Bex, & Dakin, 2008). Internal noise is likely to reflect the tuning of disparity mechanisms early in visual cortex. Physiological evidence indicates that disparity tuning varies with eccentricity. In the periphery, disparity tuning in macaque V1 is coarser and wider (Prince, Cumming, & Parker, 2002) and, in cat cortex, standard deviations in receptive field disparity increase with eccentricity, indicating that cells are less finely tuned (Joshua & Bishop, 1970). Wider tuning curves indicate less precision in response to disparity at greater eccentricities. Receptive field size also increases with eccentricity across areas V1–V4 of human visual cortex (Smith, Singh, Williams, & Greenlee, 2001). Together, these physiological data are consistent with our behavioral finding that internal noise was the main limiting factor for stereoacuity in the periphery. Less precise estimates of the disparity of each individual element would create noisier estimates of the disparity of each patch of leaves and thereby elevate depth discrimination thresholds.

Our estimates of sampling efficiency are relatively constant across the visual field. This suggests that disparity signals are not globally integrated to extract the mean depth, which would compensate for an increase in external noise once external noise exceeds the level of internal noise in the visual system. Disparity pooling has been suggested as a means of cancelling out spurious disparity signals (Fleet, Wagner, & Heeger, 1996; Tyler & Julesz, 1980); however, it does not appear to be used to compensate for increased levels of noise to

judge the average depth of clustered elements at different disparities. However, perceptual disparity averaging is known to occur over a small spatial range. Parker and Yang (1989) constructed random dot patterns with alternating rows of dots at different depths. The stimulus was perceived at the mean disparity of the two component depths only when the disparity difference was within 114 arcsec. This type of disparity averaging is not present in the dead leaves stimulus used here as it appeared as a patch of ellipses at different depths rather than as a thickened surface at a single mean disparity. The lack of global integration of local estimates in stereoacuity is in contrast to the extraction of global motion direction. In central vision, Dakin, Mareschal, and Bex (2005a) found that the number of pooled local estimates of motion direction increased when more elements were added to the display, evidence that the motion system is efficient at pooling local estimates to extract a global direction of motion. There does not appear to be an analogous pooling process in the extraction of disparity. This may be because, in order to extract fine disparity differences between the two eyes, the visual system already integrates over a large spatial extent by cross correlation (e.g., Tyler & Julesz, 1978).

The absence of a change in sampling efficiency with eccentricity is congruent with the results of Harris and Parker (1992) on the efficiency of stereopsis in random-dot stereograms. Compared to an ideal observer, human observers were found to use a limited number of dots from the total number in a stereogram for judgments of a depth discontinuity. Stereoscopic efficiency was around 20% for low numbers of dots and dropped further when more dots were added to the stimulus with efficiency reaching as low as 0.5–2% when the number of dots exceeded 150. Harris and Parker (1992) calculated that observers never used more than five dots at the depth discontinuity to make their judgment. The present experiment extends this to the periphery. Across the visual field, the number of elements observers used to make the depth discrimination remained static even though each stimulus contained 200 ellipses. Indeed, the estimates of N we obtained were very low across all eccentricities: $N \approx 1$ for JC and SG, and $N \approx 4$ for observer SW who was highly practiced on the task. Together, these data indicate that the stereo efficiency of observers is consistently very low across the visual field, and thus the reduction in stereoacuity with eccentricity cannot be due to any change in sampling efficiency. This observation is directly analogous to motion processing in the peripheral visual field (Mareschal, Bex, & Dakin, 2008) where sampling efficiency is also relatively invariant of eccentricity.

An important consideration is whether the increase in internal noise relates to monocular or binocular processes. Positional acuity is also known to degrade with eccentricity, even for stimuli equated for visibility (Waugh & Levi, 1993). It is possible that the increase in internal noise observed in the periphery for depth discrimination could be explained by increased positional uncertainty. For vernier acuity, Levi and Waugh (1994) found that peak masking spatial frequency varied with eccentricity; the masking function peaked at lower spatial scales for greater eccentricities and higher spatial frequencies in the fovea, suggestive of a change in spatial scale across the visual field. Levi and Waugh (1994) found that the shift in scale did not completely account for the decline in positional acuity in the periphery as the thresholds fell faster than the change in peak spatial frequency masking. It is unclear whether local estimates of disparity are noisier in the periphery because of greater positional uncertainty (a monocular cause) or because of binocular processes involving disparity detectors.

Summary and conclusions

Observers were able to discriminate the depth of two patches of "dead leaves" stimuli containing ellipses varying in orientation, luminance, size, and disparity—even at relatively high levels of disparity noise (up to $SD = 13.56$ arcmin). Stereoacuity declined with eccentricity; thresholds for depth discrimination were on average around 5 times higher at the furthest peripheral location tested (9°) compared to the fovea. Equivalent noise analysis revealed that this decline is exclusively due to an increase in internal noise in the peripheral visual field with no change in sampling efficiency. Sampling efficiency remained very low across the visual field. When external noise exceeded internal noise, thresholds were proportional to the level of noise in the stimulus, thus the stereo system was not able to compensate by increasing sampling efficiency to "average out" the noise. An increase in internal noise with eccentricity is consistent with physiological findings of broader disparity tuning and larger receptive field size in the periphery. We conclude that reduced stereoacuity in the periphery is a result of a loss of precision in local disparity estimates early in depth processing.

Acknowledgments

This work was supported by NIH EY018664 and EY019281 awarded to Peter Bex and a Campbell Perry International Research Scholarship from the Universi-

ty of Sydney and an Australian Postgraduate Award awarded to Susan Wardle.

Commercial relationships: none.
Corresponding author: Susan G. Wardle.
Email: swardle@psych.usyd.edu.au.
Address: School of Psychology, The University of Sydney, Sydney, New South Wales, Australia.

References

Allard, R., & Faubert, J. (2006). Same calculation efficiency but different internal noise for luminance- and contrast-modulated stimuli detection. *Journal of Vision, 6*, 322–334, http://www.journalofvision.org/content/6/4/3, doi:10.1167/6.4.3. [PubMed] [Article].

Aschenbrenner, C. M. (1954). Problems in getting information into and out of air photographs. *Photogrammetric Engineering, 20*, 398–401.

Barlow, H. B. (1956). Retinal noise and absolute threshold. *Journal of the Optical Society of America, 46*, 634–639. [PubMed].

Blakemore, C. (1970). The range and scope of binocular depth discrimination in man. *The Journal of Physiology,* 211, 599–622. [PubMed].

Brainard, D. H. (1997). The psychophysics toolbox. *Spatial Vision, 10,* 433–436. [PubMed].

Cormack, L. K., Stevenson, S. B., & Schor, C. M. (1991). Interocular correlation, luminance contrast and cyclopean processing. *Vision Research, 31,* 2195–207. [PubMed].

Curcio, C. A., & Allen, K. A. (1990). Topography of ganglion cells in human retina. *The Journal of Comparative Neurology, 300*, 5–25. [PubMed].

Curcio, C. A., Sloan, K. R., Kalina, R. E., & Hendrickson, A. E. (1990). Human photoreceptor topography. *The Journal of Comparative Neurology, 292*, 497–523. [PubMed].

Dakin, S. C., Bex, P. J., Cass, J. R., & Watt, R. J. (2009). Dissociable effects of attention and crowding on orientation averaging. *Journal of Vision, 9*(11):28, 1–16, http://www.journalofvision.org/content/9/11/28, doi:10.1167/9.11.28. [PubMed] [Article].

Dakin, S. C., Mareschal, I., & Bex, P. J. (2005a). Local and global limitations on direction integration assessed using equivalent noise analysis. *Vision Research, 45*, 3027–3049. [PubMed].

Dakin, S. C., Mareschal, I., & Bex, P. J. (2005b). An oblique effect for local motion: Psychophysics and natural movie statistics. *Journal of Vision, 5*(10):9, 878–887, http://www.journalofvision.org/content/5/10/9, doi:10.1167/5.10.9. [PubMed] [Article].

Fendick, M., & Westheimer, G. (1983). Effects of practice and the separation of test targets on foveal and peripheral stereoacuity. *Vision Research, 23*, 145–150. [PubMed].

Fleet, D. J., Wagner, H., & Heeger, D. J. (1996). Neural encoding of binocular disparity: Energy models, position shifts and phase shifts. *Vision Research, 36,* 1839–1857. [PubMed].

Harris, J. M., & Parker, A. J. (1992). Efficiency of stereopsis in random-dot stereograms. *Journal of the Optical Society of America A, 9,* 14–24. [PubMed].

Heeley, D. W., Buchanan-Smith, H. M., Cromwell, J. A., & Wright, J. S. (1997). The oblique effect in orientation acuity. *Vision Research, 37*, 235–242. [PubMed].

Howard, H. J. (1919). A test for the judgment of distance. *Transactions of the American Ophthalmological Society, 17,* 195–235. [PubMed] [Article].

Jennings, J. A., & Charman, W. N. (1981). Off-axis image quality in the human eye. *Vision Research, 21*, 445–455. [PubMed].

Joshua, D. E., & Bishop, P. O. (1970). Binocular single vision and depth discrimination. Receptive field disparities for central and peripheral vision and binocular interaction on peripheral single units in cat striate cortex. *Experimental Brain Research, 10*, 389–416. [PubMed].

Julesz, B. (1971). *Foundations of cyclopean perception*. Chicago: University of Chicago Press.

Langer, M. S. (2008). Surface visibility probabilities in 3D cluttered scenes. *Computer Vision—ECCV 2008, 5302,* 401–412.

Lee, A., Mumford, D., & Huang, J. (2001). Occlusion models for natural images: A statistical study of a scale-invariant dead leaves model. *International Journal of Computer Vision, 41*, 35–59.

Levi, D. M., Klein, S. A., & Aitsebaomo, A. (1985). Vernier acuity, crowding and cortical magnification. *Vision Research, 25*, 963–977. [PubMed].

Levi, D. M., & Waugh, S. J. (1994). Spatial scale shifts in peripheral vernier acuity. *Vision Research, 34*, 2215–2238. [PubMed].

Lindgren, J. T., Hurri, J., & Hyvärinen, A. (2008). Spatial dependencies between local luminance and contrast in natural images. *Journal of Vision, 8*(12):6, 1–13, http://www.journalofvision.org/content/8/12/6, doi:10.1167/8.12.6. [PubMed] [Article].

Liu, Y., Bovik, A. C., & Cormack, L. K. (2008). Disparity statistics in natural scenes. *Journal of Vision, 8*(11):19, 1–14, http://www.journalofvision.org/content/8/11/19, doi:10.1167/8.11.19. [PubMed] [Article].

Lu, Z. L., & Dosher, B. A. (1999). Characterizing human perceptual inefficiencies with equivalent internal noise. *Journal of the Optical Society of America A, 16*, 764–778. [PubMed].

Mareschal, I., Bex, P., & Dakin, S. (2008). Local motion processing limits fine direction discrimination in the periphery. *Vision Research, 48*, 1719–1725. [PubMed].

McKee, S., Bravo, M., Taylor, D., & Legge, G. (1994). Stereo matching precedes dichoptic masking. *Vision Research, 34*, 1047–1060. [PubMed].

McKee, S. P. (1983). The spatial requirements for fine stereoacuity. *Vision Research, 23*, 191–198. [PubMed].

Nakayama, K., & Shimojo, S. (1992). Experiencing and perceiving visual surfaces. *Science, 257*, 1357–1363. [PubMed].

Ogle, K. N., & Weil, M. P. (1958). Stereoscopic vision and the duration of the stimulus. *Archives of Ophthalmology, 59,* 4–17. [PubMed].

Olmos, A., & Kingdom, F. A. A. (2004). A biologically inspired algorithm for the recovery of shading and reflectance images. *Perception, 33*, 1463–1473. [PubMed].

Parker, A. J., & Yang, Y. (1989). Spatial properties of disparity pooling in human stereo vision. *Vision Research, 29,* 1525–1538. [PubMed].

Pelli, D. G. (1997). The VideoToolbox software for visual psychophysics: Transforming numbers into movies. *Spatial Vision, 10,* 437–442. [PubMed].

Prince, S. J. D., Cumming, B. G., & Parker, A. J. (2002). Range and mechanism of encoding of horizontal disparity in macaque V1. *Journal of Neurophysiology, 87*, 209–221. [PubMed].

Rawlings, S. C., & Shipley, T. (1969). Stereoscopic acuity and horizontal angular distance from fixation. *Journal of the Optical Society of America, 59*, 991–993. [PubMed].

Rovamo, J., Virsu, V., & Näsänen, R. (1978). Cortical magnification factor predicts the photopic contrast sensitivity of peripheral vision. *Nature, 271*, 54–56. [PubMed].

Ruderman, D. L. (1997). Origins of scaling in natural images. *Vision Research, 37*, 3385–3398. [PubMed].

Siderov, J., & Harwerth, R. S. (1995). Stereopsis, spatial frequency and retinal eccentricity. *Vision Research, 35*, 2329–2337. [PubMed].

Smith, A. T., Singh, K. D., Williams, A. L., & Greenlee, M. W. (2001). Estimating receptive field size from fMRI data in human striate and extrastriate visual cortex. *Cerebral Cortex, 11,* 1182–1190. [PubMed].

Snyder, A. (1982). Hyperacuity and interpolation by the visual pathways. *Vision Research, 22*, 1219–1220. [PubMed].

Solomon, J. A. (2010). Visual discrimination of orientation statistics in crowded and uncrowded arrays. *Journal of Vision, 10*(14):19, 1–16, http://www.journalofvision.org/content/10/14/19, doi:10.1167/10.14.19. [PubMed] [Article].

Srivastava, A., Lee, A., Simoncelli, E., & Zhu, S. (2003). On advances in statistical modeling of natural images. *Journal of Mathematical Imaging and Vision, 18*, 17–33.

Stevenson, S. B., Cormack, L. K., & Schor, C. M. (1989). Hyperacuity, superresolution and gap resolution in human stereopsis. *Vision Research, 29*, 1597–1605. [PubMed].

Tyler, C. W., & Julesz, B. (1978). Binocular cross-correlation in time and space. *Vision Research, 18,* 101–105. [PubMed].

Virsu, V., Näsänen, R., & Osmoviita, K. (1987). Cortical magnification and peripheral vision. *Journal of the Optical Society of America A, 4*, 1568–1578. [PubMed].

Virsu, V., & Rovamo, J. (1979). Visual resolution, contrast sensitivity, and the cortical magnification factor. *Experimental Brain Research, 37*, 475–494. [PubMed].

Wardle, S. G., Cass, J., Brooks, K. R., & Alais, D. (2010). Breaking camouflage: Binocular disparity reduces contrast masking in natural images. *Journal of Vision, 10*(14):38, 1–12, http://www.journalofvision.org/content/10/14/38, doi:10.1167/10.14.38. [PubMed] [Article].

Waugh, S. J., & Levi, D. M. (1993). Visibility, luminance and vernier acuity. *Vision Research, 33,* 527–38. [PubMed].

Westheimer, G. (1975). Editorial: Visual acuity and hyperacuity. *Investigative Ophthalmology, 14,* 570–572. [PubMed] [Article].

Westheimer, G. (1979). Cooperative neural processes involved in stereoscopic acuity. *Experimental Brain Research, 36*, 585–597. [PubMed].

Westheimer, G., & McKee, S. P. (1979). What prior uniocular processing is necessary for stereopsis?

Investigative Ophthalmology & Visual Science, 18, 614–621. [PubMed] [Article].

Westheimer, G., & McKee, S. (1980a). Stereoscopic acuity with defocused and spatially filtered retinal images. *Journal of the Optical Society of America, 70*, 772–778.

Westheimer, G., & McKee, S. P. (1980b). Stereogram design for testing local stereopsis. *Investigative Ophthalmology & Visual Science, 19*, 802–809. [PubMed] [Article].

Wilson, J. R., & Sherman, S. M. (1976). Receptive-field characteristics of neurons in cat striate cortex: Changes with visual field eccentricity. *Journal of Neurophysiology, 39*, 512–533. [PubMed].